

A multi-objective optimization approach for harnessing rainwater in changing climate

Meng, Ling Yu; Tian, Zhan; Fan, Dong Li; van de Ven, Frans H.M.; Sun, Laixiang; Ye, Qing Hua; Sun, San Xiang; Liu, Jun Guo; Nougues, Laura; Rooze, Daan

DOI

[10.1016/j.accre.2024.08.006](https://doi.org/10.1016/j.accre.2024.08.006)

Publication date

2024

Document Version

Proof

Published in

Advances in Climate Change Research

Citation (APA)

Meng, L. Y., Tian, Z., Fan, D. L., van de Ven, F. H. M., Sun, L., Ye, Q. H., Sun, S. X., Liu, J. G., Nougues, L., & Rooze, D. (2024). A multi-objective optimization approach for harnessing rainwater in changing climate. *Advances in Climate Change Research*, 15(5), 976-987.
<https://doi.org/10.1016/j.accre.2024.08.006>

Important note

To cite this publication, please use the final published version (if applicable).
Please check the document version above.

Copyright

Other than for strictly personal use, it is not permitted to download, forward or distribute the text or part of it, without the consent of the author(s) and/or copyright holder(s), unless the work is under an open content license such as Creative Commons.

Takedown policy

Please contact us and provide details if you believe this document breaches copyrights.
We will remove access to the work immediately and investigate your claim.



A multi-objective optimization approach for harnessing rainwater in changing climate

Ling-Yu MENG^a, Zhan TIAN^{b,c,*}, Dong-Li FAN^{a,**}, Frans H.M. VAN DE VEN^{d,e}, Laixiang SUN^f, Qing-Hua YE^d, San-Xiang SUN^g, Jun-Guo LIU^b, Laura NOUGUES^d, Daan ROOZE^d

^a School of Chemical and Environmental Engineering, Shanghai Institute of Technology, Shanghai 201418, China

^b Guangdong Provincial Key Laboratory of Soil and Groundwater Pollution Control, School of Environmental Science and Engineering, Southern University of Science and Technology, Shenzhen 518055, China

^c Pengcheng Laboratory, Shenzhen 518000, China

^d Deltares, Delft 2629 HV, Netherlands

^e Water Management, Faculty of Civil Engineering and Geosciences, Delft University of Technology, Delft 2628 CN, Netherlands

^f Department of Geographical Sciences, University of Maryland, Maryland 20742, United States

^g School of Environmental and Municipal Engineering, Lanzhou Jiaotong University, Lanzhou 730070, China

Received 2 March 2024; revised 21 May 2024; accepted 15 August 2024

Abstract

As the world grapples with the profound impacts of climate change, water scarcity has become a pressing issue. However, there is a shortage of in-depth research on the trade-offs between water resource dependence and the economic, ecological, and social needs of arid and semi-arid regions like Lanzhou, China. Flower cultivation in Lanzhou relies heavily on the Yellow River, often overlooking the potential of natural rainfall. Here we first calibrated a water balance model through artificial precipitation experiments in a Soil and Water Conservation Demonstration Park in Lanzhou. We then developed a multi-objective optimization model to balance the cost-benefit considerations of various plausible measures across economic, ecological, and social dimensions in the searching for solutions that are more adaptable to climate change and local development needs. Model simulations show that the solutions we designed can effectively manage water-shortage days, significantly reduce Yellow River water extraction, and improve cost-effectiveness, meeting 66%–80% of water needs for flower cultivation in the studied park. The findings highlight the potential of rainwater collection and utilization solutions to mitigate water scarcity in arid and semi-arid cities, thereby enriching water resource management.

Keywords: Rainwater harvesting; Rainwater resource utilization; Climate change adaptation; Multi-objective decision making; Arid and semi-arid regions

1. Introduction

Extensive research on climate change highlights a global trend towards more frequent and intense droughts (Cook et al., 2020). This phenomenon is particularly pronounced in

Northwestern China, where severe drought and water scarcity are increasingly critical challenges (Mekonnen and Hoekstra, 2016; Liu et al., 2017; Zhang et al., 2022). Lanzhou, the biggest city in northwestern China, is particularly affected, with its flower cultivation heavily reliant on the Yellow River while

* Corresponding author. Guangdong Provincial Key Laboratory of Soil and Groundwater Pollution Control, School of Environmental Science and Engineering, Southern University of Science and Technology, Shenzhen 518055, China.

** Corresponding author.

E-mail addresses: tianz@sustech.edu.cn (TIAN Z.), fandl@sit.edu.cn (FAN D.-L.).

Peer review under responsibility of National Climate Centre (China Meteorological Administration).

<https://doi.org/10.1016/j.accre.2024.08.006>

1674-9278/© 2024 The Authors. Publishing services by Elsevier B.V. on behalf of KeAi Communications Co. Ltd. This is an open access article under the CC BY-NC-ND license (<http://creativecommons.org/licenses/by-nc-nd/4.0/>).

neglecting the potential of natural rainfall. The overexploitation of Yellow River water resources has resulted in reduced water availability and deteriorating water quality, impacting the ecological balance (Gu et al., 2019; Wei et al., 2023). Recent policies have emphasized the need to reduce dependency on Yellow River water, promoting green and sustainable development (Xi, 2019; Sullivan, 2023). This shift provides new perspectives for arid and semi-arid regions, suggesting that rainwater collection and utilization can alleviate water scarcity (Zhang et al., 2021; El-Rawy et al., 2023; Umukiza et al., 2023).

Many studies have focused on the impact of rainwater utilization on reducing flood risks and enhancing drought resilience (Campisano et al., 2017; de Sá Silva et al., 2022). In arid regions where precipitation is relatively scarce, greater attention should be paid to the potential benefits of enhancing drought resilience. Analyzing the spatiotemporal distribution of regional precipitation helps in understanding the relationship between rainwater collection and domestic water consumption, thereby achieving temporal alignment of water supply and demand (Aladenola and Adeboye, 2010). In the agricultural sector, rainwater utilization can supplement water-deficient plants or irrigation for surrounding agriculture, thereby increasing food production in arid regions (Meskele et al., 2023; Zheng et al., 2023). Additionally, studies have designed optimal rainwater tank sizes to ensure meeting anticipated needs even during dry months (Imteaz et al., 2012; Lopes et al., 2017). Therefore, implementing rainwater harvesting technology for flower cultivation sustains growth during low rainfall months and reduces reliance on Yellow River water, alleviating water resource pressures and promoting ecological conservation.

Rainfall harvest is regarded as an effective way to bridge the mismatch between water demand and local rainfall patterns, and it is important to incorporate climate change into the design of rainwater harvesting solutions. Adaptations specific to each location, such as adjusting tank size, catchment area, or water demand, are necessary to ensure a sustainable water supply under future climate conditions. Previous studies have predominantly based the design and assessment of rainwater harvesting solutions on historical rainfall data (Jing et al., 2018; Maqsoom et al., 2021; Teston et al., 2022). However, these studies have not fully informed users about the expected performance of rainwater harvesting solutions under future rainfall conditions (Zhang et al., 2019; Rahmat et al., 2020). This lack of awareness may lead to disparities between expected outcomes and actual solution performance. Recent studies have utilized data from stochastically-generated models or general circulation models (GCMs) to design and evaluate rainwater harvesting solutions (Ali et al., 2021; Imteaz et al., 2021; Islam et al., 2021), providing a more accurate assessment of their effectiveness under changing climate conditions.

The utilization of rainwater resources largely depends on site conditions such as precipitation, catchment area (Jing et al., 2018), tank size (Xie et al., 2023), and water demand (Raimondi et al., 2023). Several studies have collected data from different locations and evaluated performances of various rainwater sourcing scenarios including tank size, irrigation area, and building occupancy (di Matteo et al., 2019; Crosson

et al., 2021). Economic and ecological cost-benefit analyses are typically required to support the feasibility of solutions determined by design methodologies. Trade-offs between conflicting objectives may arise, for instance, meeting user water demand might necessitate large tank sizes, thereby increasing construction and maintaining costs. Combining hydrological modeling with multi-objective optimization methods is considered as an effective approach (Lopes and Silva, 2021; Yang et al., 2023). Widely used methods include ant colony optimization (ACO) (Lord et al., 2021), particle swarm optimization (PSO) (Saplioglu et al., 2019), simulated annealing (SA) (Semaan et al., 2020), and genetic algorithms (GAs) (Snir et al., 2022), with GAs being recognized for their accuracy and effectiveness.

However, studies on rainwater utilization considering climate change have typically focused on a single water conservation objective, lacking a multidimensional approach that balances economic, ecological, and societal values. Furthermore, the design of rainwater utilization solutions should take local policies and development needs into account. For instance, leveraging rainwater for flower cultivation in Lanzhou, a hub for specialized horticultural industries, aligns with policies aimed at conserving Yellow River water and promoting the development of specialized horticultural industries, thereby carrying social implications. To address these important gaps, we developed a multi-objective optimization model aiming to balance the cost-benefit considerations of various solution designs across economic, ecological, and social dimensions in the search for solutions that are more adaptable to climate change and local development needs. For the well-functioning of this optimization model, we calibrated a water balance model through artificial precipitation experiments in a Soil and Water Conservation Demonstration Park in Lanzhou. This water balance model enables us to take the uncertainty of future climate change into the solution simulation process. Our approach thus provides new perspectives for shifting resource dependence in arid and semi-arid regions.

2. Materials and methods

2.1. Study area

The study area is the Soil and Water Conservation Demonstration Park, located in the Doujia Mountain area of Chengguan district, Lanzhou city. This park is one of the main test bases for soil and water conservation (Fig. 1). The park faces great challenges of seasonal water scarcity due to limited water resources and the high complexity of constructing major water conservancy projects nearby. Precipitation is unevenly distributed throughout the year (Fig. A1), with considerable variability in certain years. The primary growing season for floral crops is from April to November, during which the monthly water demand ranges from 100 to 150 mm, exceeding the corresponding average monthly precipitation (Fig. A1). This is particularly evident in April, October, and November, reflecting an imbalance between the supply and demand of water for crop growth (Liao et al., 2006; Jin et al., 2017).

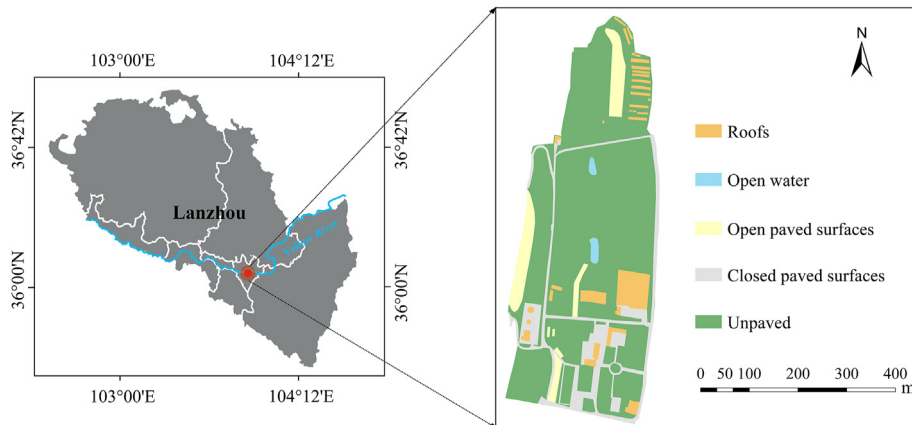


Fig. 1. The study area.

2.2. Data

2.2.1. Observation records

Daily precipitation (mm), maximum and minimum temperature ($^{\circ}\text{C}$), relative humidity (%), sunshine hours (h), and wind speed (m s^{-1}) over 1954–2020 at the Yuzhong station were obtained from China Meteorological Data Network (<https://data.cma.cn/metadata>). The reference evapotranspiration (ET_0) (mm) was calculated using this meteorological data and the FAO Penman-Monteith equation. ET_0 represents the evapotranspiration rate from a reference grass surface with ample water supply (Allen et al., 1998, 2006; Howell and Evett, 2004). For more details, please refer to Appendix. Elevation and land use data were obtained through field measurements conducted during June–December 2021.

2.2.2. Experimental data

Artificial precipitation experiments were conducted to provide the water balance model with data on initial losses and infiltration losses. A total of 48 precipitation scenarios were designed, encompassing eight different surface types (loess with 0%, 50%, and 75% weed cover, lawns, compacted loess, cement soil, permeable bricks, and concrete) and six precipitation intensities (0.41, 0.71, 0.92, 1.20, 1.54, and 1.89 mm min^{-1}) over a 60-min artificial storm duration. Soil moisture content, soil infiltration rate, total runoff volume, runoff intensity, and the start and end times of runoff were measured using both manual and automatic methods (Text A2; Fig. A2).

2.2.3. Projection data

Future precipitation and evapotranspiration in 2041–2070 were generated based on the Earth System Model (EC-Earth3) (Döscher et al., 2022) in the sixth phase of the Coupled Model Intercomparison Project (CMIP6) under SSP126, SSP245, and SSP585 scenarios.

2.3. Water balance model

To study the dynamic behavior of water resources and flows in the area and the retention tanks, this study employed the

urban water balance model (UWBM) (Deltares, 2020a, 2020b). This open-source, lumped hydrological model includes the hydrological processes and climate characteristics relevant in the northwest region of China. The UWBM simulates urban hydrological processes such as precipitation runoff from roofs, impervious surfaces, previously paved and unpaved surfaces, saturated and unsaturated shallow groundwater, evapotranspiration, surface water, and discharge from combined or separate sewer systems. It also calculates the potential for rainwater resources utilization in different land use areas, thereby assessing the dynamic distribution of rainwater resources over time and space.

2.4. Change factor method

Due to the relatively low spatial resolution, EC-Earth3 can be imprecise in capturing regional/local-scale climate changes and often face challenges in modeling extreme weather events. A direct adoption of EC-Earth3 would lead to large uncertainty in simulating rainwater resource potential in and around the studied park. Hence, we employed the simple Change Factor Method (CFM) (Fowler and Kilsby, 2007; Prudhomme and Davies, 2009; Maraun et al., 2010). This method overlays climate warming information to study the intensity and structure of weather events under future climate change. It subtracts or compares future monthly average predictions with historical monthly climate data to derive the signal of future climate change. Observed data from Yuzhong stations are used as a reliable climate background to generate daily predictions for future climate scenarios. This method effectively retains original weather information and the frequency of extreme weather events, making the simulation results more reliable.

$$\Delta \bar{T}_{\text{month}} = \bar{T}_{\text{future,month}} - \bar{T}_{\text{historical,month}} \quad (1)$$

$$\Delta \bar{E}_{\text{month}} = \frac{\bar{E}_{\text{historical,month}}}{\bar{E}_{\text{future,month}}} \quad (2)$$

Using EC-Earth3, the monthly temperature predictions for 2041–2070 ($\bar{T}_{\text{future,month}}$) were subtracted from the historical data (1981–2010, $\bar{T}_{\text{historical,month}}$) to obtain the signal of

temperature changes ($\Delta\bar{T}_{\text{month}}$, Eq. 1). The historical monthly precipitation/radiation data from 1981 to 2010 ($\bar{E}_{\text{historical,month}}$) were divided by the future precipitation/radiation predictions from 2041 to 2070 ($\bar{E}_{\text{future,month}}$) to obtain the signal of precipitation/radiation changes (Eq. 2). The obtained monthly climate change signals were linearly interpolated to generate a collection of daily meteorological datasets (ΔT_{daily} and ΔE_{daily}), which were then multiplied (addition of temperature signals) by the observed data ($T_{\text{obs,daily}}$ and $E_{\text{obs,daily}}$) from Yuzhong stations from 1981 to 2010 to obtain a set of future daily climate scenario (Eqs. 3 and 4).

$$T_{\text{daily}} = T_{\text{obs,daily}} + \Delta T_{\text{daily}} \quad (3)$$

$$E_{\text{daily}} = E_{\text{obs,daily}} \times \Delta E_{\text{daily}} \quad (4)$$

3. Methodologies

We proposed a multi-objective optimization model that aims to balance economic–ecological–social objectives. The objective variables include cost (F_{cost}), number of water shortage days (F_{shortage}), and volume of Yellow River water withdrawal (F_{demand}) for flowers. Optimization is performed on three decision variables: the capacity of storage/reservoir (α), scale of flower cultivation (β), and extent of rainwater collection area (γ), with the aim to obtain solutions more adaptable to climate change and local development needs. The model is developed using the Matrix Laboratory (MATLAB) platform.

3.1. Objective functions

The first objective function addresses the annual water shortage days for flower cultivation (F_{shortage}). Serving as a metric for quantifying the ecological benefits of the solution, it aims to maximize benefit of flower cultivation using collected rainwater resources. This approach helps safeguard local Yellow River water resources and facilitates the transition away from dependency. F_{shortage} are primarily calculated based on rainwater potential, reservoir volume (α), and flower water demand (D_{flower}). Using the UWBM, daily rainwater potential is computed. It is then compared with the available reservoir volume; if less, it is stored, otherwise, the reservoir's capacity becomes the potential. The available volume is compared with the water demand; if less, a water shortage day is counted, otherwise, the surplus volume after deducting demand is stored in the reservoir for future use (Fig. A4).

We can evaluate the percentage of flower water demand satisfied and the amount of rainwater resource utilization through water shortage days. It is important to note that in calculating water shortage days, we did not consider the specific shortage amount on those days; instead, we assumed 100% shortage. This implies that the computed rainwater resource utilization represents the lower bound of the utilization potential, as some rainwater from certain shortage days is utilized but not accounted due to insufficient water demand.

$$P_{\text{satisfy}} = 1 - \frac{F_{\text{shortage}}}{N_{\text{cultivation}}} \times 100\% \quad (5)$$

$$V_{\text{rainwater}} = (N_{\text{cultivation}} - F_{\text{shortage}}) \times D_{\text{flower}} \quad (6)$$

Where P_{satisfy} is the percentage of flower water needs met (% of the number of days); $N_{\text{cultivation}}$ is the number of cultivation days for flowers; $V_{\text{rainwater}}$ is the utilization of rainwater resources (m^3); and D_{flower} is the daily water demand of flower cultivation ($\text{m}^3 \text{d}^{-1}$).

The second objective function (F_{cost}) considers the total cost of rainwater utilization system construction and maintenance, along with the revenue generated from the flower market. The aim is to manage the project budget and achieve higher cost-effectiveness, seeking to obtain better benefits with the lowest investment cost. The cost is based on quotations from engineering cost provided by consulting agencies and adjusted with the actual market prices in Lanzhou. Due to the substantial difference between total investment cost and revenue, for the sake of result presentation, we calculated the negative of the difference, known as negative cost–benefit (NCB).

$$F_{\text{cost}} = (C_1\alpha + C_2\beta - C_3\gamma) \times N \quad (7)$$

Where F_{cost} is the NCB (CNY); C_1 is the unit volume cost of the reservoir (CNY m^{-3}), assuming a unit construction cost of approximately 2000 CNY m^{-3} and a unit maintenance cost of approximately 100 CNY m^{-3} per year; α is the size of the reservoir construction (m^3); C_2 is the unit area cost of the rainwater catchment area (CNY m^{-2}). Rainwater catchment area refers to surfaces designed to collect rainwater, typically constructed with low permeability materials like concrete. We enhanced rainwater harvesting potential by increasing impermeable surfaces, assuming a unit construction cost of approximately 100 CNY m^{-2} and a unit maintenance cost of approximately 5 CNY m^{-2} per year; β is the size of the rainwater catchment area (m^2); C_3 is the profit per flower production in a greenhouse, assuming each greenhouse has an actual flower cultivation area of approximately 200 m^2 , and the selling price is approximately 30 CNY m^{-2} based on the market price in 2023. The flowers can be harvested three times a year; γ is the scale of cultivated flowers (greenhouse); and N is the number of years.

The third objective function (F_{demand}) considers the volumes of annual Yellow River water withdrawal for each greenhouse (m^3 per greenhouse). It serves as a metric to quantify the social benefits of the solution, aiming to minimize the use of Yellow River water when collected rainwater resources are insufficient to meet the water demand. This action aligns with policies promoting reduced dependence on Yellow River water, thereby fostering societal environmental awareness. It is primarily related to the γ and F_{shortage} . Rational planning of flower cultivation scale contributes to the development of the local floral industry, facilitating job creation, enhancing cultural identity among residents, and fostering tourism development.

$$F_{\text{demand}} = \frac{F_{\text{shortage}} \times D_{\text{flower}}}{\gamma} \quad (8)$$

3.2. Decision variables

The decision variables α and β are subject to the engineering standards (GB/T 50596–2010) and actual land usage. Construction sizes should be below allowable total volume/area and exceed existing reservoir volume, in increments of 10. γ abides by industry planning and land usage. F_{cost} is capped at 5 million CNY, following specific constraint equation:

$$\begin{cases} a_1 \leq \alpha \leq b_1, \alpha \in 10 \times N \\ \beta \leq \beta_{\text{max}}, \beta \in 10 \times N \\ a_2 \leq \gamma \leq b_2, \gamma \in N \\ F_{\text{cost}} \leq 5 \times 10^6 \end{cases} \quad (9)$$

Where a_1 is the minimum prescribed reservoir size (m^3) and is set to 50 m^3 ; b_1 is the maximum prescribed reservoir size (m^3)

and is set to 500 m^3 ; β_{max} is the maximum prescribed catchment area (m^2) and is set to $100,000 \text{ m}^2$; a_2 is the minimum prescribed cultivated scale (greenhouse) and is set to 5 greenhouses; b_2 is the maximum prescribed cultivated scale (greenhouse) and is set to 100 greenhouses.

3.3. Optimization algorithm

Advanced data analysis techniques, particularly Pareto multi-objective optimization, are frequently used to determine the optimal solutions (Hallegatte et al., 2012).

Among existing algorithms for Pareto-optimal solution sets, Non-dominated Sorting Genetic Algorithm (NSGA) is regarded as advanced. NSGA-II (Deb et al., 2000), an enhancement of NSGA, introduces an elitist strategy. It generates offspring via selection, crossover, and mutation, merging with parents. Swift non-dominated sorting and crowding distance computation maintain elite parent individuals and convergence on the Pareto front. This boosts efficiency and reduces computational time. NSGA-II parameters follow Yao

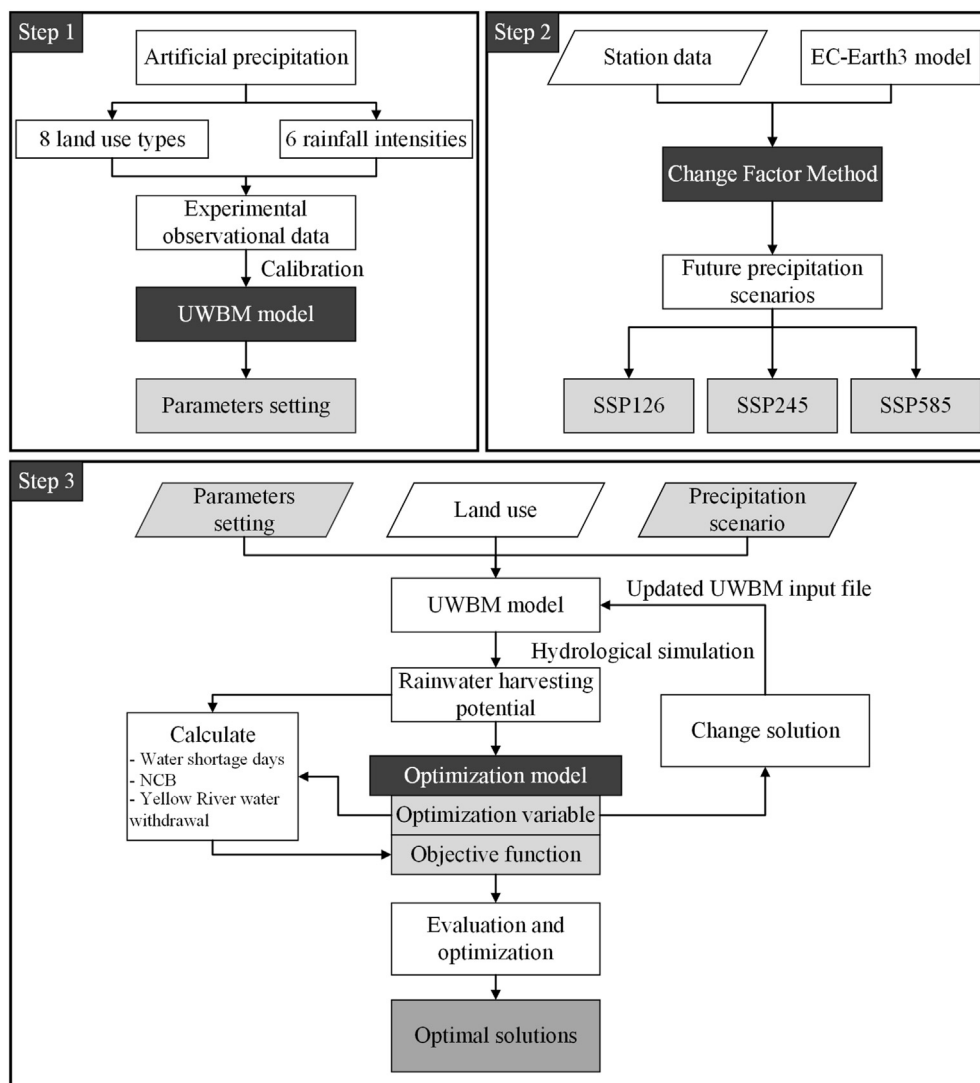


Fig. 2. Technical route.

et al. (2022) and Liu et al. (2019): population size 50, generations 400, crossover probability 1.0, mutation probability reciprocal of length.

3.4. Linkage of NSGA-II to the UWBM model

The process of the optimization model is summarized as follows, depicted in step 3 of Fig. 2. Firstly, the UWBM model is established based on the actual situation, and then a large number of optimization solutions are generated using the optimization model, each of which contains size information of different optimization variables. The generated optimization variables are written into .ini files using MATLAB (.ini can be processed by the UWBM) and the UWBM model is run to obtain new simulation results. The return value is calculated by the objective function and fed back to the optimization model for evaluation and then optimization in the next iteration. The optimization results are obtained through multiple iterations until the modeling process is completed.

To identify feasible optimal solutions, a detailed analysis of the Pareto optimal set involves assigning weights to each objective function variable for calculating the highest comprehensive score. The entropy weight method (EWM) (Li et al., 2011; Delgado and Romero, 2016), a prevalent multi-criteria decision-making technique, is employed for weight determination. EWM employs information entropy to allocate weights based on the relative information discreteness of variables, with higher weights signifying greater discreteness (Text A3).

3.5. Technical route

As depicted in Fig. 2, we began by processing and analyzing fundamental data including precipitation, evaporation, and land use. The UWBM is employed to conceptualize the study area, calibrated using observed results. Subsequently, the Change Factor Method (CFM) generates projections for 2041–2070. Coupling the UWBM with NSGA-II, we created an economic–ecological–social multi-objective optimization model that balances the minimization objectives.

4. Results

4.1. UWBM calibration

The calibration parameters for the UWBM can be categorized into three groups. The first group pertains to interception and depression storage capacity (instorcap), representing the water retained by vegetation or surface depressions intercepting rainwater (mm). The second category involves infiltration capacity (infilcap), indicating the rate at which water penetrates the soil in different zones (mm d^{-1}). The third group encompasses vegetation and soil types. Vegetation relates to predominant crop types on unpaved land, offering options like lawns, crops, and non-cultivated land. Soil type encompasses primary categories such as clay, peat soil, and sandy soil. Accurate determination of these sensitive parameters relies on monitoring specific conditions within the study area.

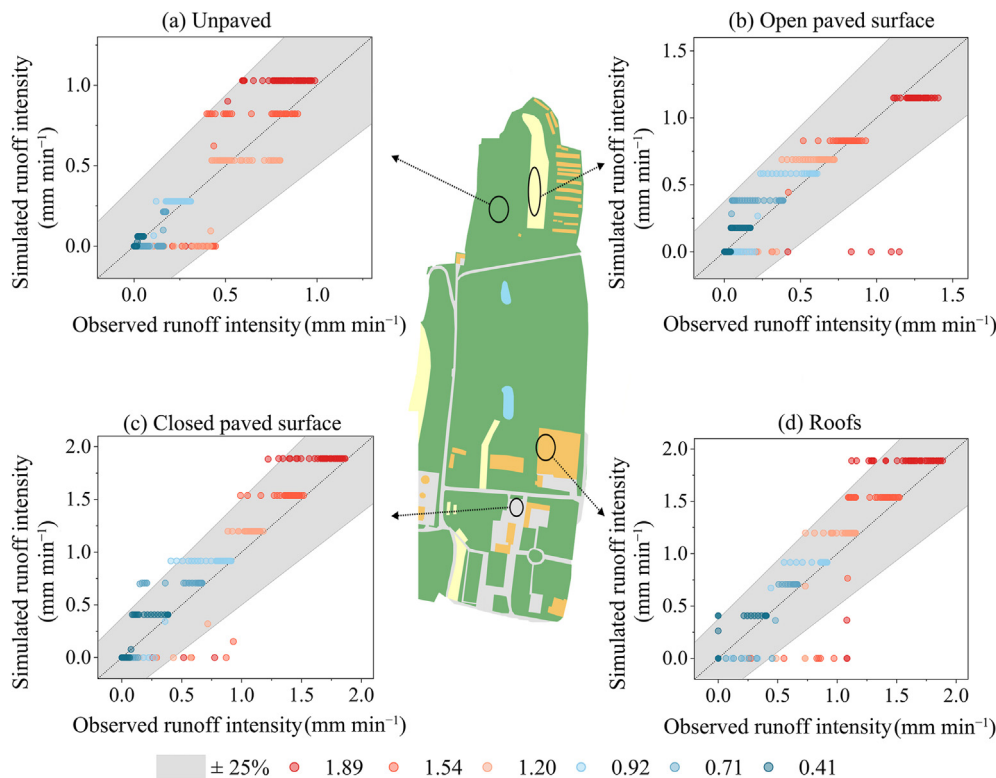


Fig. 3. Model calibration results, (a) runoff from unpaved area with 50% weed cover mirroring the current vegetation, (b) areas with permeable bricks, (c) impervious areas with concrete, and (d) cement surfaces (In the legend, $\pm 25\%$ represents the tolerance interval, with colors indicating rainfall intensity).

Calibration was performed using field experiment outcomes (Text A2; Fig. A2), local observations, and remote sensing data. The model simulated 48 precipitation scenarios, covering eight land use types and six precipitation intensities. For calibration, three intensities (0.41, 0.92, and 1.54 mm min⁻¹) were chosen for each land use type, guided by the following criteria: minimizing relative error in total simulated runoff; minimizing relative error in stable runoff intensity; and minimizing root-mean-square error (RMSE) between simulated and observed runoff. Results revealed relative errors in total simulated runoff ranging from 0% to 13.3%, relative errors in stable runoff intensity from 0% to 9.9%, and RMSE between simulated and observed runoff spanning 0.01–0.27 mm min⁻¹ (Table A2).

Post-calibration, constant model parameters were maintained, and validation utilized the remaining three intensities (0.71, 1.20, and 1.89 mm min⁻¹) for each land use type. Validation results demonstrated relative errors in total simulated runoff spanning 0.3%–27.6%, relative errors in stable runoff intensity ranging from 0% to 33.3%, and RMSE between simulated and observed runoff spanning 0.03–0.32 mm min⁻¹ (Table A3).

Fig. 3 displays the runoff comparisons across scenarios. The model performed well for precipitation intensities of 0.41, 0.71, 0.92, and 1.20 mm min⁻¹, but less accurately for 1.54

and 1.89 mm min⁻¹. The calibration results exhibit a ‘stage-like’ pattern, which is related to the calculation method used in the model. In the UWBM, runoff generation strictly adheres to the balance of precipitation minus infiltration, plant interception, and evaporation. These factors are set as constant values at the initial calculation and do not change with the hydrological process. When a constant precipitation intensity is inputted, the simulated runoff intensity remains stable (constant on the y-axis) once the soil moisture reaches saturation. However, in the artificial rainfall experiment, the infiltration rate varies with soil moisture content, and the experiment cannot achieve an ‘ideal state’ of hydrological processes. As a result, the observed runoff intensity exhibits a slower ascent due to factors such as percolation runoff and wind drift losses (fluctuations on the x-axis), contributing to the ‘stage-like’ pattern in the calibration results. We adhered to the three guiding principles outlined above to minimize errors caused by the model's calculation method.

4.2. Historical scenario simulation for 1954–2020

Based on the calibrated UWBM and historical observation data from 1954 to 2020, multi-objective optimization was performed to generate the Pareto front consisting of 50 optimal solutions, as shown in Fig. 4. The Pareto front exhibits

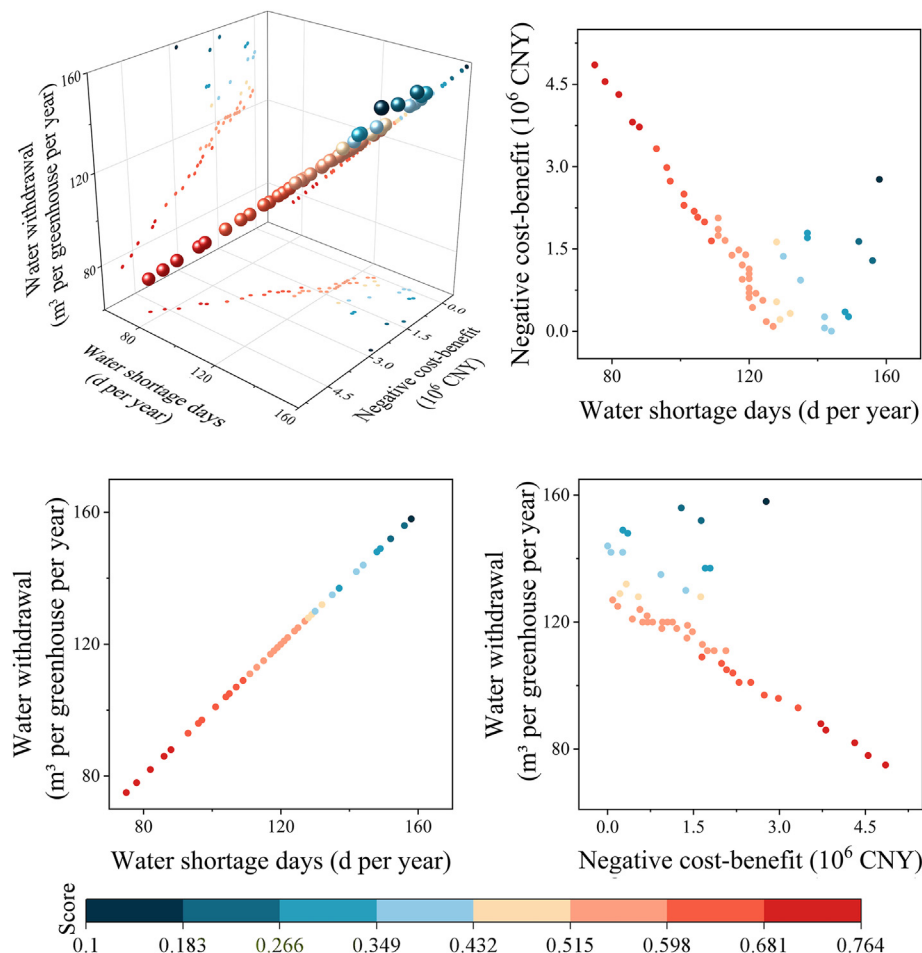


Fig. 4. Pareto optimal solutions for the 1954–2020 historical scenario simulation.

a continuous trend when projected onto the target space. The number of water shortage days positively correlates with the volume of Yellow River water withdrawal, while the NCB negatively correlates with both factors.

Fig. 4 also shows the Pareto front projection on different coordinate planes, indicating the relationship between objective function values and optimization performance. Over the past 67 years, the maximum number of water shortage days range from 75 to 158 d per year. Rainwater harvesting can satisfy approximately 35%–69% of the annual water demand of flower cultivation in the park, with a lower-bound of rainwater utilization at about 510–3010 m³ per year. Each greenhouse would require 75–158 m³ of Yellow River water per year to supplement water deficits during the periods of insufficient rainfall. The total NCB over 67 years ranges from 2850–4,850,000 CNY.

The number of water shortage days and the volume of Yellow River water withdrawal are approximately directly proportional. This indicates that as the number of water shortage days increase, the demand for water from the Yellow River per unit of flowers also increases. Conversely, the number of water shortage days and the volume of Yellow River water withdrawal are approximately inversely proportional to the NCB, respectively. A higher NCB reflects greater investment and maintenance costs, reduced number of water shortage days, and decreased volume of Yellow River water withdrawal. Conversely, a lower NCB indicates the opposite. In other words, increasing investment in construction of reservoirs and catchment area reduces the water shortage pressure in flower cultivation, thereby reducing the demand for Yellow River water and achieving the ecological conservation goals. In practical applications, different design solutions can be selected based on planning requirements.

4.3. Future simulation for 2041–2070

Utilizing the change factor method to generate precipitation and evaporation data, we quantified precipitation and non-rainy days for 2041–2070 under SSP126, SSP245, and SSP585 scenarios. A comparison with historical observational data is presented in Fig. 5.

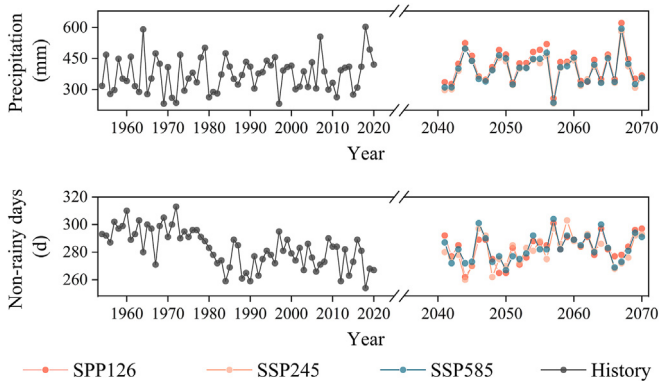


Fig. 5. Annual precipitation and non-rainy days in history (1954–2020), and SSP126, SSP245 and SSP585 scenarios for 2041–2070.

Surprisingly, our findings reveal higher annual precipitation and an increasing number of non-rainy days in future scenarios compared to historical records. This suggests a non-uniform distribution of changes in future precipitation throughout the year, leading to an increase in extreme weather events, including prolonged droughts or intense rainfall events.

Fig. 6 presents the Pareto front simulated for 2041–2070, showing the Pareto optimal solution sets under SSP126, SSP245, and SSP585 scenarios, respectively. The synthesis scenario adds the choice of SSP126, SSP245, and SSP585 as an additional decision variable in the genetic optimization algorithm (Section 3.3) so that we can evaluate the integrated Pareto optimal solution set across SSP126, SSP245, and SSP585 scenarios. For each scenario, the model generated 50 optimized solutions. Fig. 6 also shows the projections of the Pareto front on different coordinate planes.

Notably, the maximum number of water shortage days in SSP126, SSP245, SSP585, and synthesis scenarios ranges from 47 to 200, 49–204, 49–199, and 49–182 d per year, respectively. Rainwater harvesting can meet 16%–81% of the annual water demand of flower cultivation in the park, with a lower bound of rainwater utilization at 485–3740 m³ per year.

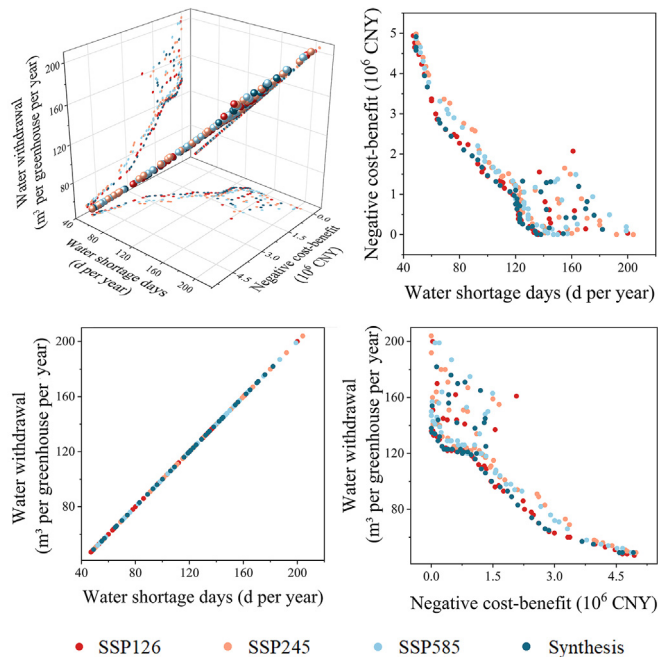


Fig. 6. Pareto optimal solutions for future scenario simulation for 2041–2070, and the synthesis scenario (The synthesis scenario adds the choice of SSP126, SSP245, and SSP585 as an additional decision variable in the optimization algorithm).

Table 1 Evaluation indicator weights on each objective under different scenarios.

| Scenario | $F_{shortage}$ | F_{cost} | F_{demand} |
|------------------------|----------------|------------|--------------|
| Historical observation | 0.381 | 0.237 | 0.381 |
| SSP126 | 0.291 | 0.418 | 0.291 |
| SSP245 | 0.340 | 0.321 | 0.340 |
| SSP585 | 0.355 | 0.290 | 0.355 |
| Future comprehensive | 0.393 | 0.214 | 0.393 |

Table 2
Pareto optimal solutions under different scenarios.

| Scenario | Solution | Reservoir size (m ³) | Cultivation scale (greenhouse) | Catchment areas (m ²) | F_{shortage} (d per year) | F_{cost} (10 ⁶ CNY) | $V_{\text{rainwater}}$ (m ³ per year) | P_{satisfy} (%) |
|------------------------|----------|----------------------------------|--------------------------------|-----------------------------------|------------------------------------|---|--|--------------------------|
| Historical observation | 1 | 500 | 5 | 15,020 | 75 | 485 | 845 | 69 |
| | 2 | 500 | 5 | 14,320 | 78 | 455 | 830 | 68 |
| | 3 | 500 | 5 | 13,780 | 82 | 431 | 810 | 66 |
| SSP126 | 4 | 490 | 5 | 12,460 | 64 | 287 | 900 | 74 |
| | 5 | 500 | 5 | 11,250 | 70 | 261 | 870 | 71 |
| | 6 | 490 | 5 | 12,990 | 63 | 300 | 905 | 74 |
| SSP245 | 7 | 490 | 5 | 17,060 | 57 | 402 | 935 | 77 |
| | 8 | 480 | 5 | 17,060 | 58 | 397 | 930 | 76 |
| | 9 | 500 | 5 | 17,500 | 56 | 418 | 940 | 77 |
| SSP585 | 10 | 490 | 5 | 16,120 | 58 | 378 | 930 | 76 |
| | 11 | 490 | 5 | 17,520 | 55 | 413 | 945 | 78 |
| | 12 | 500 | 5 | 14,050 | 66 | 331 | 890 | 73 |
| Future comprehensive | 13 | 480 | 5 | 19,510 | 49 | 458 | 975 | 80 |
| | 14 | 480 | 5 | 19,810 | 49 | 465 | 975 | 80 |
| | 15 | 480 | 5 | 15,870 | 57 | 367 | 935 | 77 |

Each greenhouse would require about 47–204 m³ of Yellow River water per year to compensate for water deficits during periods of insufficient rainfall. The total NCB over 30 years (2041–2070) may require up to 4,980,000 CNY. In practical applications, appropriate design schemes should be chosen based on specific planning requirements and considering climate change implications.

4.4. Finding the best solutions

Based on the obtained Pareto front, alternative optimal solutions can be selected according to actual needs and investment budget. To this end the weights of the variables in the objective function are assessed using the EWM. The resulting weights of the variables are shown in Table 1.

Across five scenario conditions, F_{cost} exhibit relatively smaller weights compared to the other two indicators, suggesting a lesser influence on overall solution scores (Text A3, Table 1). However, This does not diminish the importance of F_{cost} in solution adaptability. Furthermore, we observed equal weighting for F_{shortage} and F_{demand} , attributed to their proportional relationship in calculations (Eq. 8).

Solutions with a lower number of water shortage days and reduced volume of Yellow River water withdrawal, combined with higher cost-effectiveness, achieve high comprehensive scores, as shown in Figs. 4 and 6. The Pareto optimal set obtained from the model output is sorted using the EWM method, and the top three cases with the highest comprehensive scores are selected for further discussion (Table 2).

5. Conclusions and discussion

This study underscores the potential of strategies centered on rainwater harvesting and utilization as a solution to water scarcity. We employed artificial precipitation experiments to calibrate a water balance model and formulated future scenarios using the Change Factor Method. We developed a comprehensive optimization model, which integrate the water balance

model with the Non-Dominated Sorting Genetic Algorithm II (NSGA-II), to balance the cost-benefit considerations of various plausible measures across economic, ecological, and social dimensions. This approach seeks to develop solutions that are more adaptable to climate change and local development needs, providing new perspectives for addressing water scarcity challenges in arid and semi-arid regions.

The results indicate that constructing a 500 m³ reservoir and a catchment area of 13,800–15,000 m² can meet 66%–69% of the annual water demand of the five greenhouses in the park. The lower-bound level of rainwater utilization would be 810–845 m³ per year, and each greenhouse would require 75–82 m³ of Yellow River water per year to compensate for water deficits during periods of insufficient rainfall. Under future scenarios for 2041–2070, building a 480–500 m³ reservoir and a catchment area of 11,300–19,800 m² can meet 71%–80% of the annual water demand of the five greenhouses. The lower bound level of rainwater utilization would be 870–975 m³ per year, and each greenhouse would need 49–70 m³ of Yellow River water per year to compensate for water deficits during periods of insufficient rainfall.

The main factor leading to solution differences is varying precipitation and evaporation among scenarios. When the negative cost-benefit (NCB) is below 1,000,000 CNY, the number of water shortage days tend to be above 120 d per year. This indicates that, when considering lower investment costs, the possibility of using rainwater resources to meet the water demand of flower cultivation in the studied park is lower. Planners must balance these two objectives and consider their priorities and importance. It is important to note that the quantified indicators of economic–ecological–social benefits serve merely as numerical references. Planners still need to consider the long-term implicit returns of the solutions, including but not limited to the potential benefits of promoting the development of characteristic industries and responding to policy calls.

In the future, the increasingly pronounced uneven distribution of annual precipitation enhances the significance of

rainwater collection and utilization. Timely collection and storage of rainwater can alleviate water scarcity in arid and semi-arid regions, enabling greater flexibility to adapt to climate change and uneven precipitation. Compared to previous studies, our optimization model is able to find solutions which meet local development needs, strike a balance across economic, ecological, and social considerations, and are adaptive to future climate change. It is applicable for finding a coexistence pathway between resource dependence transition and urban development in arid and semi-arid regions. The model requires data inputs such as terrain conditions, meteorological observations, hydrological modeling, and climate change scenarios. The saved water is not confined to the Yellow River but depends on the city's resource-dependent water types, e.g., groundwater or river water, and can be utilized for purposes beyond flower cultivation, such as street cleaning and municipal greenery irrigation (Lyu et al., 2020; Butera et al., 2021; Carollo et al., 2022). Therefore, our optimization model is versatile across different scenarios and case studies, contingent upon case-specific data availability and well-defined optimization objectives.

In addition to the above numerical demonstration, this study has the following general implications. The first is about shift in resource dependency. As regions like northwestern China face increasing water scarcity due to climate change, there is a pressing need to shift from traditional water sources, like the Yellow River, to alternative and sustainable methods, such as rainwater harvesting. Second, by reducing dependence on traditional water sources and embracing efficient rainwater utilization strategies, regions can potentially decrease water-related costs. This could also boost industries, like flower cultivation in Lanzhou, by providing a more sustainable and cost-effective water source. Third, over-reliance on a single water source can have detrimental ecological impacts. By diversifying water resources, ecosystems related to traditional water sources can be better preserved. While the study focuses on Lanzhou, the methodologies and insights might be adaptable and applicable to other regions with similar challenges, driving wider policy changes and water resource management strategies. Fourth, the use of advanced modeling techniques, like NSGA-II, underlines the importance of technology in addressing contemporary environmental challenges. It suggests that continued investment in research and technology is crucial for developing future-ready solutions. Furthermore, the research underscores the importance of comprehensive studies in shaping policy directions. Authorities and stakeholders can leverage such insights to formulate informed policies, promote awareness, and drive community participation in sustainable practices.

This study offers insights into urban rainwater resource utilization at a community level but has limited consideration for urban planning and building density. The findings may not be fully transferable to the entire urban context. Additionally, the climate change scenarios obtained through Change Factor Method are relatively coarse and do not fully capture the uncertainties of future climate change. To improve accuracy,

future research could employ larger-scale simulations and more comprehensive urban factors. Moreover, exploring the relationship between urban rainwater resource utilization and sustainability could inform more rational urban planning and management strategies, fostering sustainable urban development.

Declaration of competing interest

The authors declare no conflict of interest.

CRediT authorship contribution statement

Ling-Yu Meng: Writing – original draft, Validation, Methodology, Investigation. **Zhan Tian:** Writing – review & editing, Resources, Conceptualization. **Dong-Li Fan:** Supervision, Resources. **Frans H.M. van de Ven:** Writing – review & editing, Software, Methodology. **Laixiang Sun:** Writing – review & editing, Supervision, Conceptualization. **Qing-Hua Ye:** Writing – review & editing. **San-Xiang Sun:** Data curation. **Jun-Guo Liu:** Resources. **Laura Nougues:** Software. **Daan Rooze:** Software.

Acknowledgments

The work was supported by the Shenzhen Science and Technology Program (KCXFZ20201221173412035 and JCYJ20210324104004013), the National Key R&D Program of China (2018YFE0206200), the Guangdong Provincial Key Laboratory of Soil and Groundwater Pollution Control (2023B1212060002), the Guangdong Basic and Applied Basic Research Foundation (2022A1515011070), and the High-level University Special Fund of SUSTech (G03050K001).

Appendix A. Supplementary data

Supplementary data to this article can be found online at <https://doi.org/10.1016/j.accre.2024.08.006>.

References

- Aladenola, O.O., Adeboye, O.B., 2010. Assessing the potential for rainwater harvesting. *Water Resour. Manag.* 24, 2129–2137. <https://doi.org/10.1007/s11269-009-9542-y>.
- Ali, S., Zhang, S., Chandio, F.A., 2021. Impacts of rainfall change on stormwater control and water saving performance of rainwater harvesting systems. *J. Environ. Manag.* 280, 111850. <https://doi.org/10.1016/j.jenvman.2020.111850>.
- Allen, R.G., Pereira, L.S., Smith, M., 1998. *Crop evapotranspiration: guidelines for computing crop water requirements*, 56. Food and Agriculture Organization of the United Nations.
- Allen, R.G., Pruitt, W.O., Wright, J.L., et al., 2006. A recommendation on standardized surface resistance for hourly calculation of reference ET₀ by the FAO56 Penman-Monteith method. *Agric. Water Manag.* 81, 1–22. <https://doi.org/10.1016/j.agwat.2005.03.007>.
- Butera, I., Carollo, M., Revelli, R., et al., 2021. Rainwater harvesting for home-garden irrigation: a case study in Italy. *GEAM* 81–88. <https://doi.org/10.19199/2021.163-164.1121-9041.081>.

- Campisano, A., Butler, D., Ward, S., et al., 2017. Urban rainwater harvesting systems: research, implementation and future perspectives. *Water Res.* 115, 195–209. <https://doi.org/10.1016/j.watres.2017.02.056>.
- Carollo, M., Butera, I., Revelli, R., 2022. Water savings and urban storm water management: evaluation of the potentiality of rainwater harvesting systems from the building to the city scale. *PLoS One* 17, e0278107. <https://doi.org/10.1371/journal.pone.0278107>.
- Cook, B.I., Mankin, J.S., Marvel, K., et al., 2020. Twenty-first century drought projections in the CMIP6 forcing scenarios. *Earth's Future* 8, e2019EF001461. <https://doi.org/10.1029/2019EF001461>.
- Crosson, C., Tong, D., Zhang, Y., et al., 2021. Rainwater as a renewable resource to achieve net zero urban water in water stressed cities. *Resour. Conserv. Recycl.* 164, 105203. <https://doi.org/10.1016/j.resconrec.2020.105203>.
- de Sá Silva, A.C.R., Bimbató, A.M., Balestieri, J.A.P., et al., 2022. Exploring environmental, economic and social aspects of rainwater harvesting systems: a review. *Sustain. Cities Soc.* 76, 103475. <https://doi.org/10.1016/j.scs.2021.103475>.
- Deb, K., Agrawal, S., Pratap, A., et al., 2000. A fast elitist non-dominated sorting genetic algorithm for multi-objective optimization: NSGA-II. *The Sixth International Conference Paris, the Parallel Problem Solving from Nature PPSN VI*.
- Delgado, A., Romero, I., 2016. Environmental conflict analysis using an integrated grey clustering and entropy-weight method: a case study of a mining project in Peru. *Environ. Model. Software* 77, 108–121. <https://doi.org/10.1016/j.envsoft.2015.12.011>.
- Deltares, 2020a. Urban Water Balance Model, Version 0.2.0. <https://gitlab.com/deltares/urban/urbanwb>.
- Deltares, 2020b. Urban water balance model: adaptation support tool. Deltares Public Wiki. <https://publicwiki.deltares.nl/display/AST/Urban+Water+balance+model>.
- di Matteo, M., Liang, R., Maier, H.R., et al., 2019. Controlling rainwater storage as a system: an opportunity to reduce urban flood peaks for rare, long duration storms. *Environ. Model. Software* 111, 34–41. <https://doi.org/10.1016/j.envsoft.2018.09.020>.
- Döscher, R., Acosta, M., Alessandri, A., et al., 2022. The EC-Earth3 Earth system model for the coupled model Intercomparison project 6. *Geosci. Model Dev. (GMD)* 15, 2973–3020. <https://doi.org/10.5194/gmd-15-2973-2022>.
- El-Rawy, M., Batelaan, O., Al-Arifi, N., et al., 2023. Climate change impacts on water resources in arid and semi-arid regions: a case study in Saudi Arabia. *Water* 15, 606. <https://doi.org/10.3390/w15030606>.
- Fowler, H., Kilsby, C., 2007. Using regional climate model data to simulate historical and future river flows in northwest England. *Clim. Change* 80, 337–367. <https://doi.org/10.1007/s10584-006-9117-3>.
- Gu, S., Lu, C., Qiu, J., 2019. Quantifying the degree of water resource utilization polarization: a case study of the Yellow River Basin. *J. Resour. Ecol.* 10, 21–28. <https://doi.org/10.5814/j.issn.1674-764x.2019.01.003>.
- Hallegatte, Stephane, Shah, Ankur, Brown, Casey, Robert, Lempert, Stuart, Gill, et al., Sep 1 2012. Investment Decision Making Under Deep Uncertainty -Application to Climate Change. World Bank Policy Research Working Paper No. 6193. Available at SSRN: <https://ssrn.com/abstract=2143067>.
- Howell, T., Evett, S., 2004. *The Penman-Monteith Method*, 5. USDA-Agricultural Research Service, Conservation & Production Research Laboratory, Washington, DC, pp. 14–21.
- Inteaz, M.A., Adebayo, O.B., Rayburg, S., et al., 2012. Rainwater harvesting potential for southwest Nigeria using daily water balance model. *Resour. Conserv. Recycl.* 62, 51–55. <https://doi.org/10.1016/j.resconrec.2012.02.007>.
- Inteaz, M.A., Paudel, U., Santos, C., 2021. Impacts of climate change on weather and spatial variabilities of potential water savings from rainwater tanks. *J. Clean. Prod.* 311, 127491. <https://doi.org/10.1016/j.jclepro.2021.127491>.
- Islam, M.M., Afrin, S., Tarek, M.H., et al., 2021. Reliability and financial feasibility assessment of a community rainwater harvesting system considering precipitation variability due to climate change. *J. Environ. Manag.* 289, 112507. <https://doi.org/10.1016/j.jenvman.2021.112507>.
- Jin, Y., Zhou, L., Tang, X., et al., 2017. *Research on Theoretical Innovation and Technical Integration of Rural Rainwater Harvesting and Utilization*. China Water & Power Press, Beijing.
- Jing, X., Zhang, S., Zhang, J., et al., 2018. Analysis and modelling of stormwater volume control performance of rainwater harvesting systems in four climatic zones of China. *Water Resour. Manag.* 32, 2649–2664. <https://doi.org/10.1007/s11269-018-1950-4>.
- Li, X., Wang, K., Liu, L., et al., 2011. Application of the entropy weight and TOPSIS method in safety evaluation of coal mines. *Process Eng.* 26, 2085–2091. <https://doi.org/10.1016/j.proeng.2011.11.2410>.
- Liao, Y., Pan, X., Zhang, Q., et al., 2006. Daily precipitation simulation and its application on crop production climate risk analysis. *Acta Agric. Boreali-Sinica* 52, 206–212.
- Liu, G.W.C., Chen, L., Shen, Z.Y., et al., 2019. A fast and robust simulation-optimization methodology for stormwater quality management. *J. Hydrol.* 576, 520–527. <https://doi.org/10.1016/j.jhydrol.2019.06.073>.
- Liu, J., Yang, H., Gosling, S.N., et al., 2017. Water scarcity assessments in the past, present, and future. *Earth's Future* 5, 545–559. <https://doi.org/10.1002/2016EF000518>.
- Lopes, M.D., Silva, G.B.L.D., 2021. An efficient simulation-optimization approach based on genetic algorithms and hydrologic modeling to assist in identifying optimal low impact development designs. *Landsc. Urban Plann.* 216, 104251. <https://doi.org/10.1016/j.landurbplan.2021.104251>.
- Lopes, V.A.R., Marques, G.F., Dornelles, F., et al., 2017. Performance of rainwater harvesting systems under scenarios of non-potable water demand and roof area typologies using a stochastic approach. *J. Clean. Prod.* 148, 304–313. <https://doi.org/10.1016/j.jclepro.2017.01.132>.
- Lord, S.A., Ghasabaraei, M.H., Movahedinia, M., et al., 2021. Redesign of stormwater collection canal based on flood exceedance probability using the ant colony optimization: study area of eastern Tehran metropolis. *Water Sci.* 84, 820–839. <https://doi.org/10.2166/wst.2021.273>.
- Lyu, C., Zhang, W., Ling, M., et al., 2020. Quantitative analysis of economic benefits of reclaimed water for controlling urban dust. *Environ. Geochem. Health* 42, 2963–2973. <https://doi.org/10.1007/s10653-020-00537-y>.
- Maqsoom, A., Aslam, B., Ismail, S., et al., 2021. Assessing rainwater harvesting potential in urban areas: a building information modelling (BIM) approach. *Sustainability* 13, 12583. <https://doi.org/10.3390/su132212583>.
- Maraun, D., Wetterhall, F., Ireson, A., et al., 2010. Precipitation downscaling under climate change: recent developments to bridge the gap between dynamical models and the end user. *Rev. Geophys.* 48. <https://doi.org/10.1029/2009RG000314>.
- Mekonnen, M.M., Hoekstra, A.Y., 2016. Four billion people facing severe water scarcity. *Sci. Adv.* 2, e1500323. <https://doi.org/10.1126/sciadv.1500323>.
- Meskele, D.Y., Shomere, M.W., Adi, K.A., 2023. A review on harvesting rainwater for agricultural production in the rain-fed region, Ethiopia: challenges and benefits. *Sustainable Water Resources Management* 9, 176. <https://doi.org/10.1007/s40899-023-00957-5>.
- Prudhomme, C., Davies, H., 2009. Assessing uncertainties in climate change impact analyses on the river flow regimes in the UK. Part 2: future climate. *Clim. Change* 93, 197–222. <https://doi.org/10.1007/s10584-008-9461-6>.
- Rahmat, S.N., Al-Gheethi, A.A.S., Ayob, S., et al., 2020. Development of dual water supply using rooftop rainwater harvesting and groundwater systems. *SN Appl. Sci.* 2, 1–8. <https://doi.org/10.1007/s42452-019-1862-9>.
- Raimondi, A., Quinn, R., Abhijith, G.R., et al., 2023. Rainwater harvesting and treatment: state of the art and perspectives. *Water* 15, 1518. <https://doi.org/10.3390/w15081518>.
- Saplioglu, K., Kucukerdem, T.S., Şenel, F.A., 2019. Determining rainwater harvesting storage capacity with particle swarm optimization. *Water Resour. Manag.* 33, 4749–4766. <https://doi.org/10.1007/s11269-019-02389-3>.
- Semaan, M., Day, S.D., Garvin, M., et al., 2020. Optimal sizing of rainwater harvesting systems for domestic water usages: a systematic literature review. *Resour. Conserv. Recycl.* 6, 100033. <https://doi.org/10.1016/j.resconrec.2020.100033>.
- Snir, O., Friedler, E., Ostfeld, A., 2022. Optimizing the control of decentralized rainwater harvesting systems for reducing urban drainage flows. *Water* 14, 571. <https://doi.org/10.3390/w14040571>.
- Sullivan, L.R., 2023. Tackling the environment: Xi Jinping and the pursuit of a 'beautiful China'. *J. Environ. Assess. Pol. Manag.* 25, 2350005. <https://doi.org/10.1142/S1464333223500059>.

- Teston, A., Piccinini Scolaro, T., Kuntz Maykot, J., et al., 2022. Comprehensive environmental assessment of rainwater harvesting systems: a literature review. *Water* 14, 2716. <https://doi.org/10.3390/w14172716>.
- Umukiza, E., Ntole, R., Chikavumbwa, S.R., et al., 2023. Rainwater harvesting in arid and semi-arid lands of Africa: challenges and opportunities. *Acta Scientiarum Polonorum* 22, 41–52. <https://doi.org/10.15576/ASP.FC/2023.22.2.03>.
- Wei, J., Lei, Y., Liu, L., et al., 2023. Water scarcity risk through trade of the Yellow River basin in China. *Ecol. Indic.* 154, 110893. <https://doi.org/10.1016/j.ecolind.2023.110893>.
- Xi, J., 2019. Speech on the ecological protection and high quality development of the Yellow River basin forum. *China Water Resour* 20, 1–3. <http://kns.cnki.net/KCMS/detail/detail.aspx?dbcode=CJFD&filename=RMHH201910034>.
- Xie, H., Randall, M., dos Santos, S.M., 2023. Optimization of roof coverage and tank size for integrated green roof rainwater harvesting systems: a case study. *Water Resour. Manag.* 37, 4663–4678. <https://doi.org/10.1007/s11269-023-03568-z>.
- Yang, B., Zhang, T., Li, J., et al., 2023. Optimal designs of LID based on LID experiments and SWMM for a small-scale community in Tianjin, North China. *J. Environ. Manag.* 334, 117442. <https://doi.org/10.1016/j.jenvman.2023.117442>.
- Yao, Y.T., Li, J.K., Lyu, P., et al., 2022. Optimizing the layout of coupled grey-green stormwater infrastructure with multi-objective oriented decision making. *J. Clean. Prod.* 367, 133061. <https://doi.org/10.1016/j.jclepro.2022.133061>.
- Zhang, S., Zhang, J., Yue, T., et al., 2019. Impacts of climate change on urban rainwater harvesting systems. *Sci. Total Environ.* 665, 262–274. <https://doi.org/10.1016/j.scitotenv.2019.02.135>.
- Zhang, Y., An, C.-B., Liu, L.-Y., et al., 2022. High-elevation landforms are experiencing more remarkable wetting trends in arid Central Asia. *Adv. Clim. Change Res.* 13, 489–495. <https://doi.org/10.1016/j.accre.2022.04.007>.
- Zhang, W., Sheng, J., Li, Z., et al., 2021. Integrating rainwater harvesting and drip irrigation for water use efficiency improvements in apple orchards of Northwest China. *Sci. Hortic.* 275, 109728. <https://doi.org/10.1016/j.scienta.2020.109728>.
- Zheng, X., Sarwar, A., Islam, F., et al., 2023. Rainwater harvesting for agriculture development using multi-influence factor and fuzzy overlay techniques. *Environ. Res.* 238, 117189. <https://doi.org/10.1016/j.envres.2023.117189>.